2-dimensional numerical modeling of active magnetic regeneration

Nielsen, Kaspar Kirstein; Pryds, Nini; Smith, Anders; Bahl, Christian Robert Haffenden; Hattel, Jesper Henri

Published in:
3rd International Conference on Magnetic Refrigeration at Room Temperature

Publication date:
2009

Document Version
Publisher's PDF, also known as Version of record

2-dimensional numerical modeling of Active Magnetic Regeneration

K.K. Nielsen[a,b], N. Pryds[b], A. Smith[b], C.R.H. Bahl[b], J. Hattel[a]
[a] Technical University of Denmark, Department of Mechanical Engineering
Produktionstorvet, building 425, 2800 Kgs. Lyngby, Denmark
kaki@risoe.dtu.dk
[b] Risø National Laboratory for Sustainable Energy, Technical University of Denmark
Fuel Cells and Solid State Chemistry Division
Frederiksborgvej 399, 4000 Roskilde, Denmark

ABSTRACT

Various aspects of numerical modeling of Active Magnetic Regeneration (AMR) are presented. Using a 2-dimensional numerical model for solving the unsteady heat transfer equations for the AMR system, a range of physical effects on both idealized and non-idealized AMR are investigated. The modeled system represents a linear, parallel-plate based AMR.

The idealized version of the model is able to predict the theoretical performance of AMR in terms of cooling power and temperature span. This is useful to a certain extent, but a model reproducing experiments to a higher degree is desirable. Therefore physical effects such as thermal parasitic losses have been included. Furthermore, experimentally found magnetocaloric properties are used when available, since the commonly used mean field model can be too idealized and is not always able to determine the magnetocaloric effect accurately.

In the present paper preliminary conclusions on which non-ideal physical effects are thought to be dominating considering the performance of experimental AMR are given. The modeling results are compared to experimental results from the AMR test device situated at Risø DTU, Technical University of Denmark. The experimental validation shows that using the measured magnetocaloric properties significantly improves the modeling results compared to using the mean field model.

1. INTRODUCTION

The magnetocaloric effect (MCE) provides the basic ingredient for magnetic refrigeration. The effect is observed in magnetic materials when exposed to a change in external magnetic field. The MCE is usually either observed as a change in magnetic entropy, ΔS_m (when the field is applied isothermally) or as a change in temperature, ΔT_{ad} (when the field is applied adiabatically). In addition to these two fundamental observations the specific heat, c_p is usually a strong function of both temperature and field. The MCE is typically in the range of 1-5 K / T (in terms of the adiabatic temperature change). This modest change in temperature is obviously not sufficient for applications such as domestic refrigeration etc. Therefore the successful regenerative process, Active Magnetic Regeneration (AMR), is applied for magnetic refrigeration around room temperature. AMR can be thought of as a range of coupled local thermodynamic cycles that differential elements of a regenerator go through (Rowe et al., 2003). The cycle consists of four steps. The first step is the adiabatic magnetization where the magnetocaloric material (MCM) is exposed to a magnetic field under adiabatic conditions. Second, a heat transfer fluid convectively transfers heat from the MCM to the ambient through a hot side heat exchanger – also known as the hot blow. The third step is the adiabatic demagnetization, i.e. the magnetic field is removed. The final step is the so-called cold blow where the heat transfer fluid absorbs heat from a cooling load. These four steps have the durations denoted τ_1, τ_2, τ_3 and τ_4 respectively.

During the AMR cycle a heat transfer fluid and a solid refrigerant (the MCM) exchange heat dynamically and at the same time the material properties of the MCM change as function of both temperature and magnetic field. This makes it impossible to perform an analytical analysis of the entire AMR Refrigeration (AMRR) system in terms of predicting cooling power, comparing material performance and general optimization of the design. Therefore numerical modeling – obviously in close collaboration with extensive experimental studies – is crucial for the development of AMRR.

In this work the focus is on the comparison between the modeling and the experimental results, especially showing the necessity of accurate material data. In Section 2 the model is described. The

governing equations are presented and the emphasis is put on the special features of this model as well as a discussion of how to model the MCE. Results from both modeling and experimental work are presented in Section 3. Finally, in Section 4 the impact on the modeling of the different ways of obtaining the MCE are discussed on the basis of the results presented in this paper.

2. PRESENTATION OF THE MODEL

The basics of the model are summarized in the following. For a detailed description of the model see Nielsen, et al.(2009). The geometry targeted by the model is the parallel-plate based design. The system can be either reciprocating or continuous – that is not significant for the model as such. Four domains are modeled: The heat transfer fluid, MCM plate and cold and hot heat exchangers (HEXs), which can also act as passive flow guides depending on which experiment is modeled. The solid domains are fixed with respect to each other and can be rigidly moved with respect to the fluid (in order to model fluid movement). The AMRR system is thus modeled by solving the coupled heat transfer equations for each domain through a number of time steps (and AMR cycles) until quasi-steady state is reached. The numerical discretization is done using finite differences of 2nd order and the temporal integration is done using the Alternate Direction Implicit (ADI) method, thoroughly discussed in e.g. (Hattel 2005) or (Patankar 1980). The software for implementing the solver has been written by the authors and is available in generic Fortran.

2.1. Governing equations

The coordinate system is defined so the *x*-direction is parallel to the flow and the *y*-direction is perpendicular to the plane of the magnetocaloric plates, i.e. denotes the direction of the height of the MCM plates and the fluid channel. In Figure 1 and Figure 2 the geometry is schematically described. In Bahl et al., (2008) the geometrical details of the system are thoroughly described. The total system of equations can be written as:

$$\frac{\partial T_f}{\partial t} = \frac{k_f}{\rho_f c_{p,f}} \nabla^2 T_f + q_{bd,fc} + q_{bd,fh} + q_{bd,fMCM} + q_{loss,f} - u \frac{\partial T_f}{\partial x} \tag{1}$$

$$\frac{\partial T_{MCM}}{\partial t} = \frac{k_{MCM}}{\rho_{MCM} c_{p,MCM}} \nabla^2 T_{MCM} - q_{bd,fMCM} + q_{loss,MCM} \tag{2}$$

$$\frac{\partial T_c}{\partial t} = \frac{k_c}{\rho_c c_{p,c}} \nabla^2 T_c - q_{bd,fc} + q_{loss,c} \tag{3}$$

$$\frac{\partial T_h}{\partial t} = \frac{k_h}{\rho_h c_{p,h}} \nabla^2 T_h - q_{bd,fh} + q_{loss,h} \tag{4}$$

Subscripts *f, c* and *h* denote the fluid, CHEX and HHEX domains respectively. The material properties thermal conductivity, mass density and specific heat (k, ρ and c_p) respectively, are all assumed constant except the specific heat for the MCM, which varies strongly with both temperature and magnetic field. The coupling of Eqs. (1)-(4) is implemented through the boundary heat fluxes denoted by $q_{bd,fMCM}, q_{bd,fc}$ and $q_{bc,fh}$ respectively. The heat flux terms with subscript *loss* are included as parasitic thermal losses to the ambient. These are calculated through the formulation of thermal resistances on the form:

$$q_{loss} = \frac{T - T_\infty}{\sum_i R_i}. \tag{5}$$

Here, the summation is done over the number of thermal resistances R_i experienced by each individual grid cell with temperature T. The ambient temperature is denoted T_∞. The thermal resistance is calculated on the basis of the thermal properties of the materials considered. For instance, the thermal resistance experienced by the fluid is calculated as:

$$R_{fl,total} = \frac{1/2\Delta z_f}{k_f \Delta x \Delta y} + \frac{\Delta z_{pl}}{k_{pl} \Delta x \Delta y} + \frac{1}{h_{conv} \Delta x \Delta y}. \tag{6}$$

The thickness of the fluid channel, Δz_f, and of the plastic housing Δz_{pl} have been introduced. The natural convection that transfers heat from the regenerator to the ambient is modeled through the parameter h_{conv} assumed to attain a value of 10 W/m^2 K. The last term in Eq. (1) represents the convective heat transfer. The assumed fluid flow is fully developed, incompressible and laminar. Therefore only the *x*-component of the fluid velocity is non-zero. An analytical expression for the velocity profile is straightforwardly calculated in e.g. Nielsen et al. (2009):

$$u(y) = \tilde{u}\left(\frac{6y^2}{H_{fl}^2} - 1/2\right), \tag{7}$$

where $\tilde{u}$ is the inlet velocity and H_{fl} the fluid channel height.

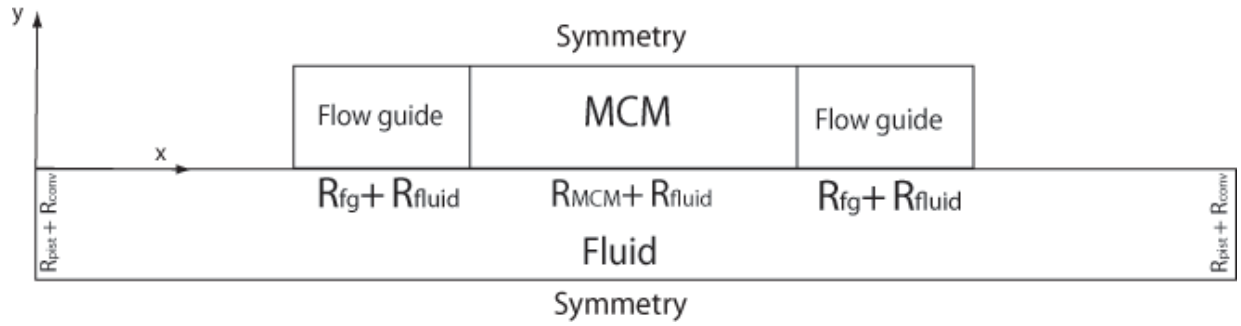

Figure 1 : The xy-plane of the regenerator model. The MCM and flow guides are fixed with respect to each other and can be moved with respect to the fluid in order to model the fluid movement. The internal boundaries are marked with their thermal resistances. The model is half a replicating cell and thus the symmetry boundaries are marked.

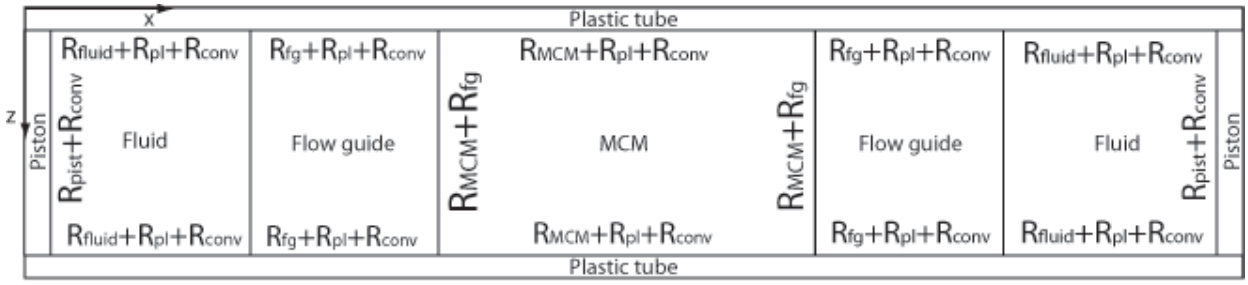

Figure 2 : The xz-plane of the regenerator model. The system should be thought of as seen from above, i.e. the fluid is hidden under the MCM and flow guides. The external boundaries are marked as the thermal resistances to the ambient. It is noted that the z-direction is not resolved by the model, but due to the thermal parasitic losses to the ambient the model can be thought of as 2.5 dimensional.

As indicated in Figure 1 the model utilizes symmetry meaning that only half a flow channel and half a MCM plate are modeled. The symmetry boundaries are by definition set so that both the heat fluxes and the fluid flow across them are zero at all times.

2.2. Obtaining the MCE

Obtaining the magnetocaloric properties of a given MCM can require some work. The well known mean field theory (MFT) (see e.g. Petersen et al. 2008, Kawanami, et al. 2006, Li, et al. 2006) is typically used when considering gadolinium (Gd). From a pure modeling point of view a nice-behaving model like the MFT is good in the sense of minimizing numerical difficulties and having a firm well-resolved data set. However, a critical view on the correspondence between MFT and experimental data should at all times be applied.

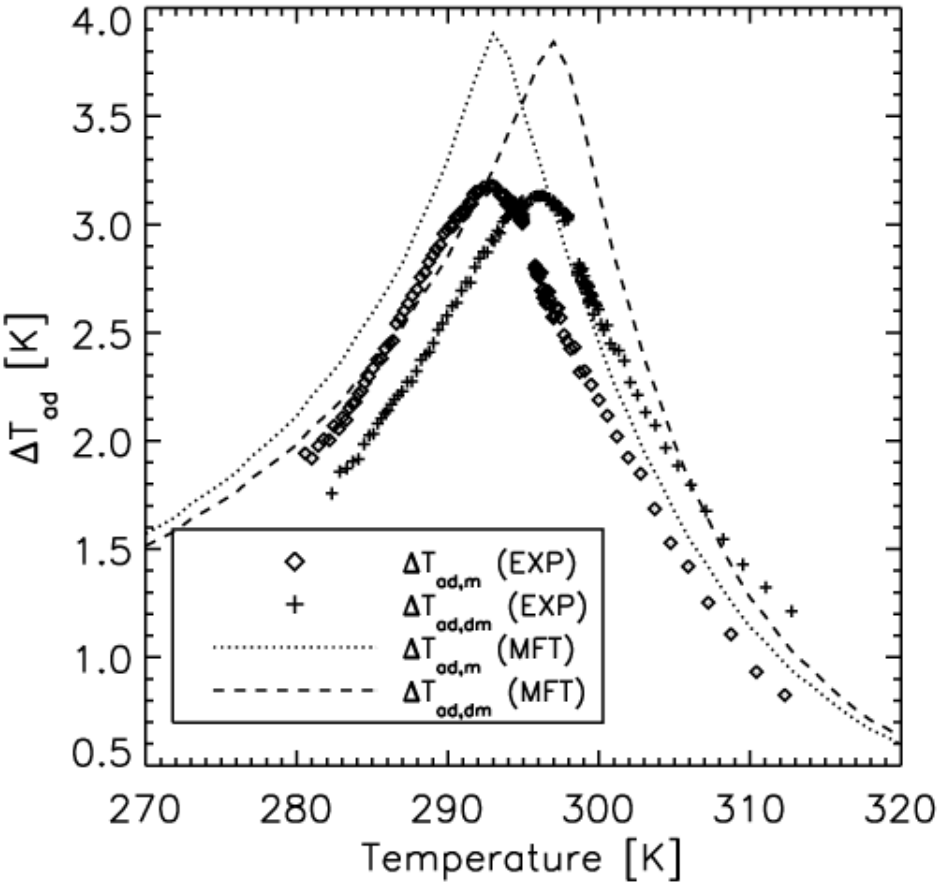

Figure 3 : The squares (magnetization) and plus-signs (demagnetization) mark experimentally obtained ΔT_{ad} values for commercial grade Gd at an applied field of approximately 1.1 T (from Bahl and Nielsen, 2009). The punctuated line (magnetization) and dashed line (demagnetization) mark the corresponding MFT based calculation. The sign of the demagnetization data reversed for clarity.

Two examples of the MFT compared with experimental data are presented in Figure 3 and Figure 4. Here the adiabatic temperature changes for Gd and the ceramic material $(La_{0.67}Ca_{0.26}Sr_{0.07})Mn_{1.05}O_3$ (LCSM) when applying a magnetic field of nearly 1.1 T are plotted. Both as calculated by the MFT and measured (the Gd data are obtained from Bahl and Nielsen (2009) and the LCSM are measured with the same technique). It seems quite evident from the figures that the MFT does not fully catch the actual adiabatic temperature change. For this there may be several explanations, of which only a few will be mentioned here. The purity of the Gd sample seems to have a large impact (Dan'kov et al. 1998). Also, demagnetization effects on the specific experiment may change the actual internal field in the sample (Bahl and Nielsen 2009). The important point is that using the MFT may be misleading if the goal is to model and precisely predict the performance of an *experimental* AMR device.

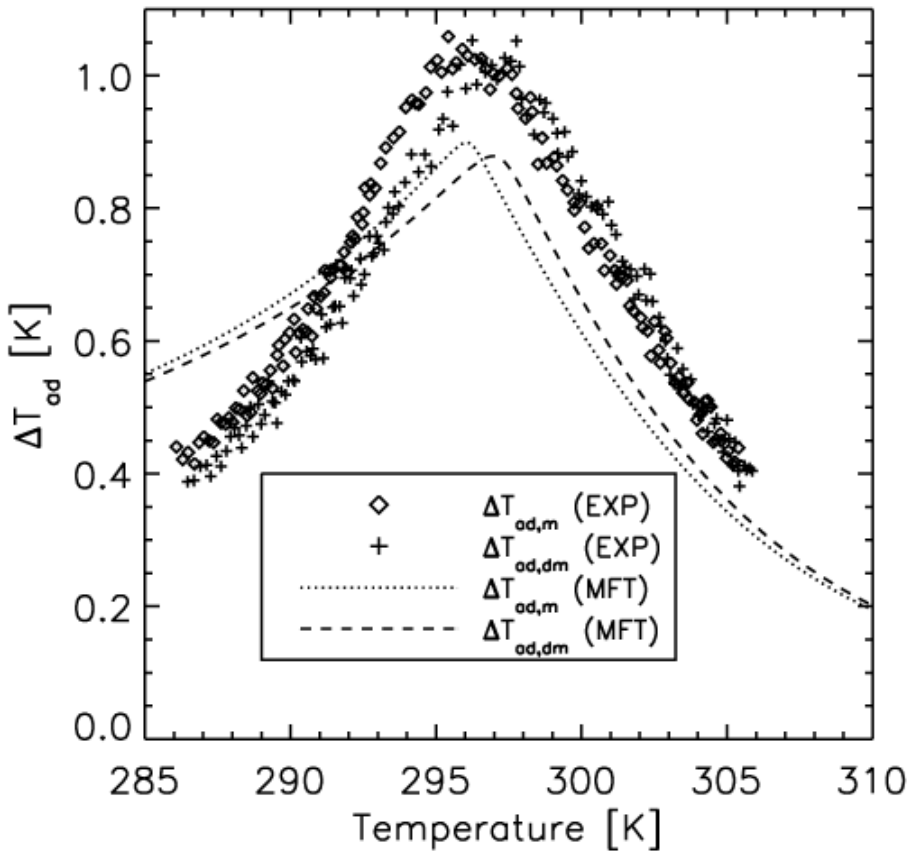

Figure 4 : The adiabatic temperature change of $(La_{0.67}Ca_{0.26}Sr_{0.07})Mn_{1.05}O_3$ both measured (using the same method as with the Gd measurements) and modeled using the MFT. The magnetic flux density of 1.1 T was applied using a Halbach permanent magnet. The input parameters for the MFT were obtained from Dinesen (2004) and are reproduced in Table 1. The sign of the demagnetization data reversed for clarity.

On the other hand, if the modeling is performed in order to predict trends and theoretically based conclusions on the ideal AMR performance, the MFT may be a wise choice. The reasons for this are, among others, that the MFT is well-behaving and thus from a numerical standpoint is easy to handle (compared to most often too insufficient data sets). It is also easier to reproduce and compare modeling across research groups compared to using a specific sample of a MCM. And finally, the MFT predicts values for both the adiabatic temperature change and specific heat capacity that are quite realistic both as function of field and temperature as would be expected of most 2nd order materials.

Table 1 : The input parameters for the mean field model as defined in e.g. Petersen et al. (2008). The parameters are (in order of appearance) number of magnetic spins per unit mass, the Landé factor, the total angular momentum, the Curie temperature, the Debye temperature, the total number of atoms per unit mass and the Sommerfeld constant. The Gd parameters are obtained from Petersen et al. (2008) while the LCSM parameters are from Dinesen (2004). It is noted that the values from Dinesen (2004) are calculated from samples with a little less Mn content (the plates used in the experiment are made of $(La_{0.67}Ca_{0.26}Sr_{0.07})Mn_{1.05}O_3$).

	$n_s\,(kg^{-1})$	g (-)	J (-)	T_c (K)	Θ_D (K)	$n\,(kg^{-1})$	$\gamma_e\,(J/kg{\cdot}K)$
Gadolinium	$3.83{\cdot}10^{24}$	2	3.5	293	169	$3.83{\cdot}10^{24}$	0.069
$(La_{0.67}Ca_{0.26}Sr_{0.07})Mn_{1.00}O_3$	$2.8{\cdot}10^{24}$	2	1.83	296	353	$1.44{\cdot}10^{25}$	0.025

3. RESULTS

The model described in the previous section can simulate a range of AMR situations. The operating parameters, fluid movement, AMR timing and ambient temperature, are easily set by input parameters. The geometric parameters (flow channel thickness, dimensions of the MCM plate) are set in the same way. The implementation of the MCE can also easily be varied between using MFT or experimental data. Likewise the thermal parameters (thermal conductivity, mass density etc.) are also provided via simple input.

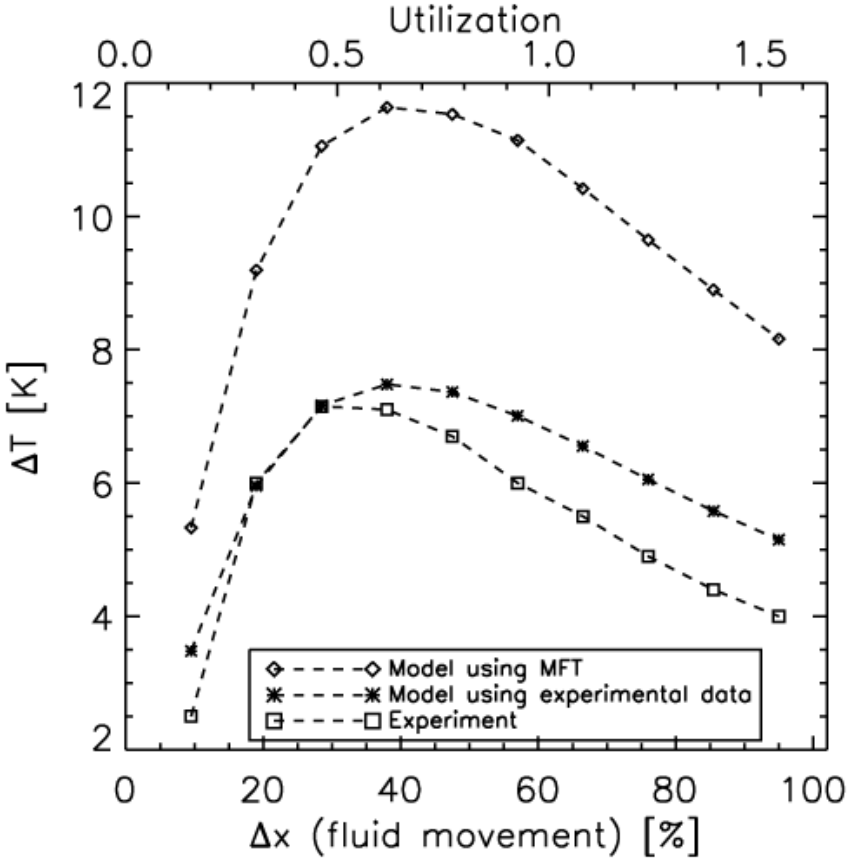

Figure 5 : The no heat load temperature span as function of fluid movement and utilization. The experiment was performed with commercial grade Gd and the parameters for both the model and experiment are given in Table 2.

The model can be set to run for a number of AMR cycles or until a steady-state has been reached. The hot and cold ends can be equipped with ideal heat exchangers (plates made of Cu with perfect contact to the ambient as first described in Petersen et al., 2008) or they can be simple fluid reservoirs in which case the rejection of heat to the ambient is only done through the thermal parasitic losses as described in Eqs. (5) and (6).

As an example we consider the effect of the implementation of the MCE. Two no heat-load experiments have been performed; one with Gd and one with LCSM (see Table 2 for details). The utilization is defined as

$$\varphi = \frac{c_{p,fl}\rho_{fl}H_{fl}}{c_{p,MCM}\rho_{MCM}H_{MCM}}\Delta x, \tag{8}$$

with Δx denoting the fluid movement in percent of the length of the MCM plate and H_{MCM} denoting the thickness of the MCM plate. The utilization can thus be adjusted by varying the amount of fluid moved. The results plotted as steady-state temperature span are given in Figure 5 and Figure 6 as function of both fluid movement and utilization. There are given two modeling situations. One using the MFT to obtain the MCE

and the other using the experimentally determined ΔT_{ad} values (plotted in Figure 3 and Figure 4 respectively). In both cases the specific heat capacity was obtained using the MFT.

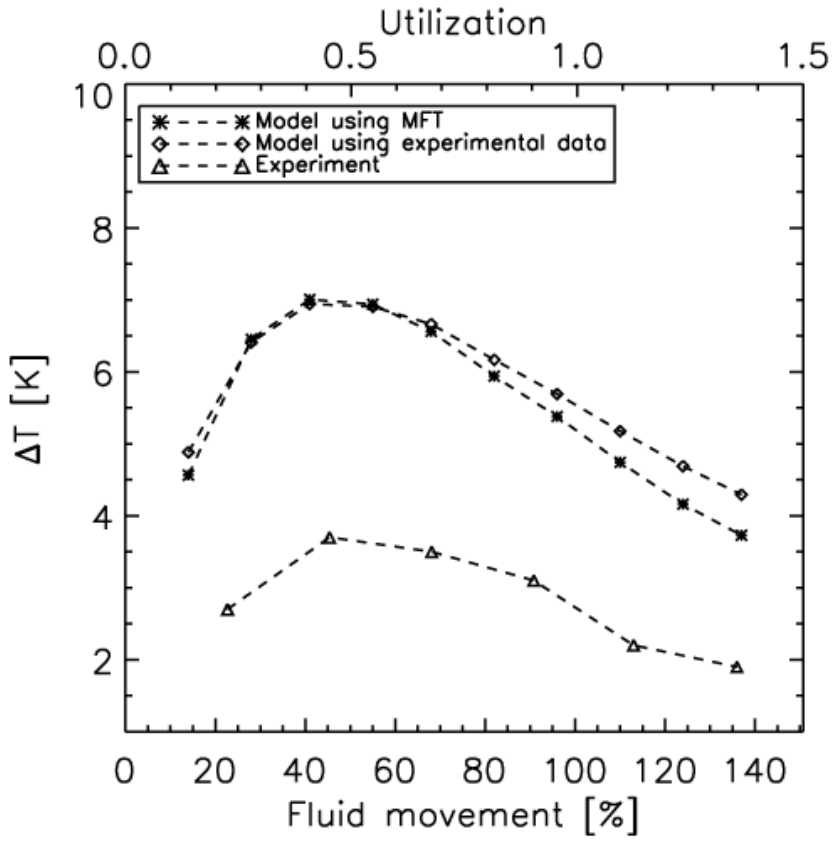

Figure 6 : Experiment with LCSM. The fluid movement has been varied (thus varying the utilization) and the modeling has been performed for two cases (one using MFT and the other experimental data for obtaining the MCE).

The results show that the model, in either case, is able to follow the tendency of the experiment, especially showing a peak value around a utilization of 0.5. It is also observed that using the experimentally determined adiabatic temperature change values significantly improves the absolute temperature span values of the model compared to the experiment when Gd is considered. This is not true for LCSM, which is also apparent from Figure 4.

Table 2 : The basic input parameters for the two experiments (and corresponding modeling). In order of appearance : The flow channel thickness, the thickness of the MCM plate, the timing of the magnetization, the timing of the hot blow and ambient temperature. Both experiments were conducted with a 1.1 T permanent magnet and with a water+ethanol mixture (10% ethanol).

	$H_{fl}(mm)$	$H_{MCM}(mm)$	$\tau_1, \tau_3(s)$	$\tau_2, \tau_4(s)$	$T_\infty(K)$
Gd	0.8	0.9	1.4	2.7	298
LCSM	0.2	0.3	1.5	1.2	296

4. CONCLUSION

An improved version of the original 2-dimensional model by Petersen et al. (2008) was presented and the concept of adding half a modeling dimension was introduced (through thermal parasitic losses to the ambient). The focus in this work was on the difference between using MFT and experimentally determined values for the MCE (considering only the adiabatic temperature change). Two different MCMs were considered, Gd and LCSM. In the case of Gd is was shown that the experimentally obtained values for the adiabatic temperature change clearly improved the correspondence of the model compared to the experiment.

In the case of LCSM the modeling results from the two cases of using MFT and experimental data respectively, were seen to be virtually the same. This was also to be expected from the presented adiabatic temperature change data in Figure 4.

Considering the usability of the MFT for obtaining the MCE as opposed to experimental data it is concluded that each individual material must be considered as a special case. For Gd the MFT may not be the best choice when modeling an actual experiment, but for LCSM the difference between the MFT and the experimentally determined adiabatic temperature change is not significant – at least in the temperature span from 285-305 K as indicated in Figure 4. In this work the specific heat capacity was as mentioned obtained using the MFT in all cases. This leaves quite some work to be done since the specific heat may deviate somewhat experimentally from that calculated using the MFT. The peak temperature may also change as function of field. This is not modeled directly through the MFT (see e.g. Tishin et al, 1999). This is a topic of big interest and therefore near-future work will include an investigation and discussion of the role of the specific heat in terms of AMR modeling – both with respect to the change in peak temperature and absolute values.

ACKNOWLEDGEMENTS

The authors thank Mr. Jørgen Geyti for his technical assistance. Furthermore the authors would like to acknowledge the support of the Programme Commission on Energy and Environment (EnMi) (Contract no. 2104-06-0032) which is part of the Danish Council for Strategic Research.

REFERENCES

Bahl, C., & Nielsen, K.K. (2009). The effect of Demagnetization on the Magnetocaloric properties of Gadolinium. *Journal of Applied Physics* . 105,013916

Bahl, C., Petersen, T., Pryds, N., & Smith, A. (2008). A versatile magnetic refrigeration test device. *Review of Scientific Instruments , 79*, 093906.

Dan'kov, S., Tishin, A., Pecharsky, V., & K.A., J. G. (1998). Magnetic phase transitions and the magnetothermal properties of gadolinium. *Physical Review B (Condensed Matter) , 57*, 3478-3490.

Dinesen, A. R. (2004). *Magnetocaloric and magnetoresistive properties of La0.67Ca0.33-xSrxMnO3.* Ph.D thesis, Technical University of Denmark.

Hattel, J. (2005). *Fundamentals of Numerical Modelling of Casting Processes.* Polyteknisk Forlag.

Kawanami, T., Chiba, K., Sakurai, K., & Ikegawa, M. (2006). Optimization of a magnetic refrigerator at room temperature for air cooling systems. *International Journal of Refrigeration , 29*, 1294-1301.

Li, P., Gong, M., Yao, G., & Wu, J. (2006). A practical model for analysis of active magnetic regenerative refrigerators for room temperature applications. *International Journal of Refrigeration , 29*, 1259-1266.

Nielsen, K.K., Bjørk, R., Bahl, C., Pryds, N., Smith, A., & Hattel, J. (n.d.). Detailed numerical modeling of a linear parallel-plate Active Magnetic Regenerator. *Submitted for publication in the International Journal of Refrigeration* .

Patankar, S. V. (1980). *Numerical Heat Transfer and Fluid Flow.* Taylor&Francis.

Petersen, T. F., Pryds, N., Smith, A., Hattel, J., Schmidt, H., & Knudsen, H. (2008). Two-dimensional mathematical model of a reciprocating room-temperature Active Magnetic Regenerator. *International Journal of Refrigeration , 31*, 432-443.

Rowe, A., & Barclay, J. (2003). Ideal magnetocaloric effect for active magnetic regenerators. *Journal of Applied Physics , 93*, 1672-1676.

Tishin, A., Gschneidner, K.A., & Pecharsky, V. (1999). Magnetocaloric effect and heat capacity in the phase-transition region. *Physical Review B (Condensed Matter) , 59*, 503-511.